Research Article

Aditya Kumar Tiwary, Harpreet Singh, Sayed M. Eldin*, and R. A. Ilyas*

Residual mechanical properties of concrete incorporated with nano supplementary cementitious materials exposed to elevated temperature

https://doi.org/10.1515/ntrev-2023-0162
received May 2, 2023; accepted November 9, 2023

Abstract: The construction industry commonly employs concrete as a construction material, which sometimes may be subjected to fire exposure. It is important to adopt fire safety measures while planning and constructing such structures to ensure the safety of the occupants and the structural integrity of the concrete. So, determining its performance at elevated temperatures is of utmost importance. The main objective of this study was to investigate the impact of mineral incorporations, namely, nano bentonite clay (NBC) and nano fly ash (NFA), on the retained properties of concrete at normal (27°C) and at elevated temperatures. The feasibility of partly substituting ordinary Portland cement utilizing a mixture of NBC (0–5%) and NFA (0–50%) in concrete was assessed under the exposure to an elevated temperature ranging from 200 to 600°C. Several parameters were examined, including compressive strength, flexural strength, split tensile capacity, water penetration, loss of mass, ultrasound pulse velocity, and microstructure properties. After the experimental analysis, it was observed that the fire endurance was shown to be improved with the inclusion of nanoparticles (BC and FA). A reduction in the loss of mass by samples subjected to elevated heat was observed with the addition of nano bentonite and NFA. The mechanical strength results were obtained as maximum for the concrete specimens with 2% NBC and 20% NFA and further, the specimens performed better when exposed to elevated temperature as compared with normal concrete specimens. The microstructure of the concrete also upgraded with better impermeability owing to the use of NBC and NFA.

Keywords: nanomaterial, elevated temperature, residual properties, microstructure analysis

Abbreviations

BC	bentonite clay
FA	fly ash
L	path length measured between transmitter and receiver (mm)
M_L	mass loss (%)
M_1	mass of concrete block before application of high temperature (kg)
M_2	mass of concrete block after application of high temperature (kg)
NBC	nano bentonite clay
NFA	nano fly ash
OPC	ordinary Portland cement
SCM	supplementary cementitious materials
SEM	scanning electron microscope
S1	concrete specimens with nano bentonite clay 1% and nano fly ash 10%
S2	concrete specimens with nano bentonite clay 2% and nano fly ash 20%

* **Corresponding author: Sayed M. Eldin,** Centre of Research, Faculty of Engineering, Future University in Egypt, New Cairo, 11835, Egypt, e-mail: sayed.eldin22@fue.edu.eg
* **Corresponding author: R. A. Ilyas,** Department of Chemical Engineering, Faculty of Chemical and Energy Engineering, Universiti Teknologi Malaysia, 81310 UTM Johor Bahru, Johor, Malaysia; Centre for Advanced Composite Materials, Universiti Teknologi Malaysia, 81310 UTM Johor Bahru, Johor, Malaysia; Institute of Tropical Forestry and Forest Products, Universiti Putra Malaysia, Serdang, 43400, Selangor, Malaysia; Centre of Excellence for Biomass Utilization, Universiti Malaysia Perlis, 02600, Arau, Perlis, Malaysia, e-mail: ahmadilyas@utm.my
Aditya Kumar Tiwary: Department of Civil Engineering, University Institute of Engineering, Chandigarh University, Mohali, 140413, Punjab, India; University Center for Research and Development, Chandigarh University, Mohali, 140413, Punjab, India, e-mail: adadtiwary15@gmail.com
Harpreet Singh: Department of Civil Engineering, University Institute of Engineering, Chandigarh University, Mohali, 140413, Punjab, India, e-mail: harpreethiharpreet@gmail.com

S3 concrete specimens with nano bentonite clay 3% and nano fly ash 30%
S4 concrete specimens with nano bentonite clay 4% and nano fly ash 40%
S5 concrete specimens with nano bentonite clay 5% and nano fly ash 50%
T_L time over which ultra-sonic pulse transits the path length (μs)
UPV ultrasonic pulse velocity
V ultra-sonic pulse velocity (km/s)
XRD X-ray diffraction

1 Introduction

Concrete is well known for having integrated fire resistance and offering some degree of endurance and thermal resistance in high-temperature scenarios. During its lifetime, infrastructure may be exposed to a number of hazards, including fire [1]. The durability of a concrete structure allows it to endure catastrophes like accidental fires for a longer period than a metallic structure. Degradation of concrete takes place owing to exposure to fire for long duration and maximum temperature. The mechanical properties of concrete can also be influenced by other attributes, namely, the heating rate, kind of aggregate, specimen size, water content, and maturity of the specimen [2–4]. As the temperature increases, water evaporates from the calcium-silicate-hydrate (CSH) paste, causing the calcium hydroxide and calcium aluminate to decompose [5,6]. Approximately 100°C is the temperature where free water evaporates, 400–500°C is the temperature when Portlandite ($Ca(OH)_2$) dehydroxylate and calcium oxide (CaO) decompose, and 600°C is the temperature at which the aggregates become quartz [7,8]. As concrete is extensively utilized in construction, determining its performance at elevated temperatures is of utmost importance [9,10].

According to Chen *et al.* [11], factors such as duration, peak temperature, and sort of cooling affect the strength of concrete. In early-stage curing, concrete that has been exposed to greater heating in the range of 800°C can regain its compressive strength. The coolant type (air/water) has an effect on the strength recovery [12]. Coskun and Tanyildizi studied the compressive and splitting tensile capacity of lightweight concrete in relation to fly ash (FA) content (10–30%) and the application of heat varying from 200 to 800°C [13]. Specimens that contained 30% FA demonstrated the most remarkable strength results. In the outcome, owing to the pozzolanic characteristics of FA, high temperatures did not adversely affect the concrete strength [14]. According to Xu *et al.* [15], high-temperature durability and mechanical characteristics of pulverized FA concrete improved under temperature ranges of 450–650°C, with 450°C having the most significant impact. In a study by Marzouk and Hussein [16], concrete containing 25% FA was tested under a wide range of temperature exposure between 21 and 232°C. For the heat application of temperatures of around 121–149°C, concrete strength was observed to be boosted. Concrete containing bentonite content was tested at ambient temperature and elevated temperature by Ahmad *et al.* Nonetheless, not much enhancement in compressive strength with bentonite content was registered. An acid attack resistance was found to be better when 30% bentonite was present [17]. Further, the compressive strength of concrete increased when bentonite content was 20% of the mix [18]. The ideal quantity of bentonite in the concrete exposed to higher temperatures is not yet fully understood. Bentonite clay (BC) is a clay material with a high montmorillonite quantity in addition to being a nano clay [19]. Nano bentonite clay (NBC) has been found to possess a greater surface area along with a greater cation exchange capacity, which makes it an effective material for use in concrete as a substitute for cement [20,21]. Further, the nano size of NBC can be very effective in filling voids which can further improve the workability, durability, and impermeability of concrete.

There is a great deal of interest in substituting pozzolanic supplementary cementitious materials (SCMs) for cement due to its high demand as a primary building material, its greater expense when compared to other ingredients in concrete, and the issues related to the release of greenhouse gases over its production. Pozzolanic materials typically have micron-sized particles; however, it is possible to crush and pulverize them to create nanoscale particles [22]. Using SCMs, such as bagasse ash [23,24], blast furnace slag [25,26], FA, and rice husk ash [27,28], in concrete production can improve its mechanical and durability performance while simultaneously reducing resource consumption and lowering carbon dioxide emissions. Silica fume enhances concrete residual strength up to 200°C; however, it causes a considerable decrease in strength at higher temperatures due to the denser transition zone [29]. The strength of FA-based concrete declined up to 250°C, then recovered between 250 and 350°C. Beyond 350°C, the FA concrete lost its strength, exhibiting superior heat resistance at 550°C than the control concrete [30]. Concrete strength with 0 and 20% ground granulated blast furnace slag (GGBFS) declined at 100°C but increased as the temperature increased. Up to 350°C, concrete with 40 and 50% GGBFS replacement ratios exhibited no significant change in residual strength, but higher replacement ratios resulted in lower strength [31]. Furthermore, alternative materials such as polypropylene

fibres [9], steel fibres [32], carbon nanotubes [33], nano silica, nano titanium [34–36], and nano alumina [37] have been employed in the production of concrete. Although these materials are effective in improving the performance of concrete in terms of mechanical and durability properties, the cost of these materials is a concern. The waste materials from industries can be utilized, which possess some cementitious properties, as partial replacement for cement for achieving cost effectiveness along with improving the mechanical and durability performance of concrete [38–40]. A reduction in carbon dioxide emissions can be achieved by replacing cement with NBC and nano fly ash (NFA) as these are obtained from waste materials and reduce the consumption of cement which is responsible for greenhouse gas emissions during its production, making concrete production more cost-effective [41,42]. Prior studies had explored the characteristics of mortar and concrete when incorporating bentonite and FA as constituents. Several experiments have presented an outcome that FA and bentonite can upgrade cementitious materials' pore structure, thus improving their durability [17,43,44].

The necessity for particular research on adding nano bentonite and NFA is a gap in the existing literature on concrete subjected to extreme temperatures. The study covers a major knowledge gap by considering fire scenarios and sustainable needs in construction, offering vital information for building fire-resistant structures and satisfying industry sustainability targets. The aim of this study is to investigate the impact of mineral incorporations, namely, NBC and NFA, on the retained properties of concrete at normal (27°C) and at elevated temperatures. In this exploration, the feasibility of partly substituting ordinary Portland cement (OPC) utilizing a mixture of NBC and NFA in concrete was considered. Mixtures included 1, 2, 3, 4, and 5% NBC with 10, 20, 30, 40, and 50% NFA. A post-fire exposure behaviour on the retained characteristics of concrete including NBC and NFA was investigated at an elevated temperature of 200, 300, 400, 500, and 600°C. Several parameters were examined, including compressive strength, flexural strength, split tensile strength, water permeability, mass loss, ultrasound pulse velocity, and scanning electron microscopy (SEM).

The present investigation examines a unique strategy to lessen the adverse consequences of high temperatures by incorporating NBC and NFA into concrete. By enhancing the thermal stability and mechanical properties of concrete, these nanoparticles have the capability to increase a structure's fire resistance and durability performance [22,42]. In the area of civil engineering, this study is crucial because it may help in the production of more durable and environmentally friendly building materials that are capable of sustaining high temperatures. Through the use of these ingredients, the investigation encourages lessening the environmental effect of usual cement production. The novel feature of this approach is the opportunity to investigate the synergistic impacts of NBC and NFA on the residual mechanical characteristics of concrete after high-temperature exposure. Through thorough investigation and evaluation, the research seeks to provide the basis for future developments in fire-resistant building materials while also offering insightful information on the effectiveness of nano-modified concrete.

2 Experimental work

2.1 Material properties

2.1.1 Cement

OPC 43 grade in compliance with IS 8112:2013 [45] was utilized as a binder for concrete production since it is the most popular kind of binder which is being utilized for the

Figure 1: Basic ingredients of concrete (a) cement, (b) fine aggregates, (c) coarse aggregates.

Table 1: Physical characteristics of coarse aggregates

Particulars	Value
Water absorption (%)	0.81
Crushing strength (%)	16.9
Loose bulk density (kg/m^3)	1,325
Rodded bulk density (kg/m^3)	1,455
Impact resistance (%)	18.6
Abrasion resistance (%)	25.8

purpose of concrete production. OPC 43 grade with a specific gravity of 3.15 and an initial setting time of 35 min as depicted in Figure 1(a) was used in this study.

2.1.2 Fine aggregate

Fine aggregate having a specific gravity of 2.65 with sand sieved over an IS 4.75 mm sieve in compliance with grading zone II of IS 383:2016 [46] as presented in Figure 1(b) was utilized in this study. Differences in void content can result in significant differences in water demand between fine aggregates of the same grading [47,48]. It is more important to consider water requirements than physical packing in determining the optimal gradation of fine aggregate for concrete. It is preferable to use fine aggregates with fineness moduli of 2.5–3.2.

2.1.3 Coarse aggregateand cooling procedure

A local quarry crushed angular granite aggregates with a nominal size of 10–20 mm and a specific gravity of 2.74 as presented in Figure 1(c) was utilized for the present investigation. Particle size distribution, water absorption, crushing strength of aggregates, bulk density, impact resistance of aggregates, and aggregate abrasion value were determined as shown in Table 1. The particle size distribution curve for fine and coarse aggregates is depicted in Figure 2(a).

2.1.4 Nanomaterials

The NBC is used in this study as shown in Figure 3(a). NBC can be used in cement by way of a binding agent in addition to enhancing the properties of the final product. When added to cement, NBC can increase the mixture's workability and flow in addition to decreasing the water content required for mixing. It can also improve the durability as well as the strength of the cement through the decrease in permeability in addition to increased resistance to chemical and physical stress [49,50]. Additionally, NBC can reduce the amount of shrinkage and cracking that occurs during the drying process. Overall, the use of NBC in cement can lead to higher quality and a more reliable final product [42].

Pulverized coal is burned in electric generation power plants to generate FA, a fine powder as shown in Figure 3(b). FA is a pozzolanic material which is composed of siliceous and aluminous compounds and can react with water to form cementitious compounds. Due to its low embodied energy as well as its role as a by-product, FA is accepted as an eco-friendly material [51]. Many FA sources contain pozzolanic FA, which consists of siliceous alumina and siliceous material that combines with calcium hydroxide to form cement [52]. The physical and chemical composition of cementitious material (NBC and NFA) is listed in

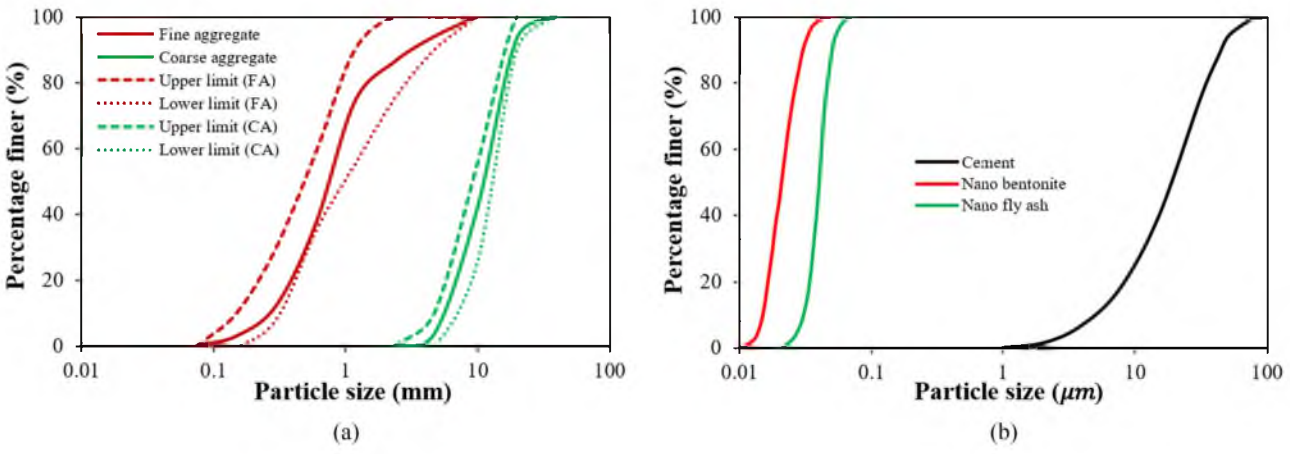

Figure 2: Particle size distribution curves (a) fine aggregate and coarse aggregate, (b) cement, NBC and NFA.

(a) (b)

Figure 3: Nanomaterials (a) NBC, (b) NFA.

Tables 2 and 3. The particle size distribution curve for cementitious materials is presented in Figure 2(b).

2.1.5 X-ray diffraction (XRD) analysis of nanomaterials

The crystallographic structure, chemical content, and physical properties of a material can all be determined by XRD analysis, a non-destructive approach. For this purpose, some samples of FA and BC have been processed into nano-form and tested using XRD. Figure 4(a–d) displays the crystalline phase of the materials that have been identified.

A peak value pointing toward the existence of chemical constituents such as calcium, magnesium, aluminium silicate, and silicon oxide in both FA and BC is depicted in Figure 4(a) and (c). Similarly, as displayed in Figure 4(b) and (d) NFA and NBC possessed the same peaks of chemical constituents. Silicon dioxide (SiO_2), aluminium oxide (Al_2O_3), iron oxide (Fe_2O_3), CaO, and a few other insignificant elements constitute a significant portion of NFA. Montmorillonite, a form of clay substance, constitutes the majority of bentonite. It additionally comprises a variety of minerals including calcite, gypsum, quartz, and feldspar. The part substitution of cement utilizing NFA and NBC is possible and it can further improve concrete's mechanical and durability properties.

Table 2: Physical characteristics of cementitious ingredients

Particulars	Cement	NFA	NBC
Specific gravity	3.15	2.1	2.3
Specific surface area (m^2/g)	0.3	360	465
Particle size (μm)	16.03	0.02–0.07	0.01–0.05

2.2 Mix design and specimen details

The concrete blend was prepared in accordance with IS 10262:2009 [53] using the procedure demonstrated in Figure 5. A total of six mixes (S0, S1, S2, S3, S4, and S5) were prepared in this study in the proportion of 1:1.7:2:48 which was determined from the mix design of M25 grade of concrete. S0 is prepared as a reference or control specimen without any addition of nanomaterials. Further, as observed in prior research, NFA significantly influences the properties of concrete when added in the proportions of 10–40% [22,54–56]. However, in the case of NBC, due to its finer particles, it might reduce the workability and can have negative effects on strength development when utilized at higher proportions, that is why lower percentages of up to 5% replacement were utilized similar to past studies to get a better insight about its behaviour in concrete [42,57,58]. Hence the other five mixes represent the samples with part substitution of cement by weight with nano bentonite in proportions of 1, 2, 3, 4, and 5%, and NFA in percentages of 10, 20, 30, 40, and 50%. The water-

Table 3: Chemical compositions of cementitious ingredients

Particulars	Cement	NFA	NBC
CaO	60.65	1.74	1.97
SiO_2	19.21	53.41	50.95
Al_2O_3	4.99	24.62	19.60
Fe_2O_3	4.11	13.12	5.62
MgO	3.02	1.22	3.29
SO_3	2.44	0.22	—
Na_2O	0.31	0.35	0.98
K_2O	0.38	0.72	0.86
TiO_2	—	1.47	0.62
MnO	—	0.1	—
P_2O_5	—	—	1.28
Loss on ignition (%)	1.65	0.5	15.45

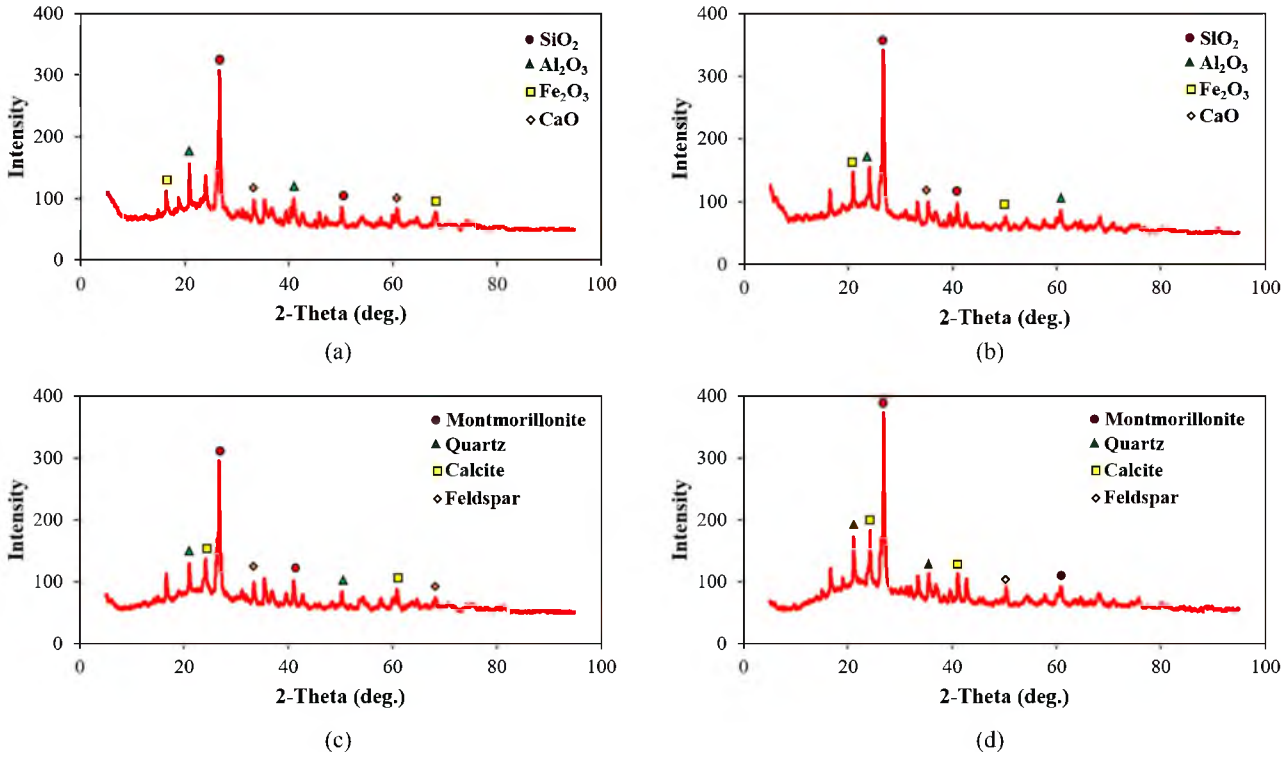

Figure 4: XRD graphs (a) fly ash, (b) NFA, (c) bentonite clay, (d) NBC.

to-cement proportion was determined as 0.42. The mix quantities for concrete specimens with NBC and NFA are depicted in Table 4.

The mix was prepared as per the proportion specified and filled in the cube (150 mm side), beam (100 mm square side and 500 mm length), and cylinder (150 mm diameter and 300 mm height) moulds. The concrete was filled in three layers with the packing of each layer through a vibrating table. An overall of 432 samples were cast comprising 216 cubes, 108 cylinders, and 108 beam specimens. Out of these, 72 specimens were set as control specimens which were tested at room temperature including 12 specimens without any utilization of NFA and NBC. For each proportion of the sample of concrete, three repetitions were made and average results were collected for the same. The description of the specimens is presented in Table 5. After filling the moulds with the concrete mix, the moulds were enfolded with a thin polythene sheet to eliminate the decrease in water content [59,60]. After the period of 24 h, the specimens were taken out from the moulds and kept inside the curing tank for 28 days which was maintained at ambient temperature [47,61]. The

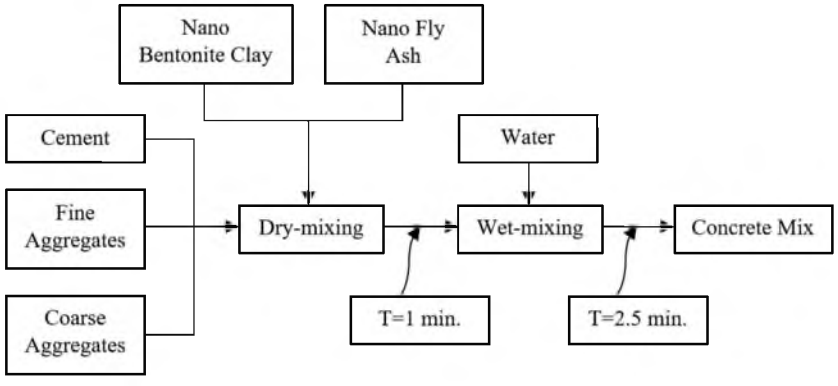

Figure 5: Concrete mixing procedure.

Table 4: Mix proportions for concrete with NBC and NFA

Samples	Cement (kg/m^3)	NFA (kg/m^3)	NBC (kg/m^3)	Fine aggregate (kg/m^3)	Coarse aggregate (kg/m^3)	Water (kg/m^3)
S0	417.00	0	0	1113.12	787.65	175.14
S1	371.13	41.7	4.17	1113.12	787.65	175.14
S2	325.26	83.4	8.34	1113.12	787.65	175.14
S3	279.39	125.1	12.51	1113.12	787.65	175.14
S4	233.52	166.8	16.68	1113.12	787.65	175.14
S5	187.65	208.5	20.85	1113.12	787.65	175.14

mixing of specimens, casted specimens and curing of specimens are displayed in Figure 6.

2.3 Heating and cooling procedure

Figure 7 shows an electric furnace possessing the ability to heat the specimens up to 1,150°C. The inner dimensions of the furnace were measured as 500 × 500 × 600 mm. Special trolleys were used to place the concrete samples inside the furnace. The heat was increased by closing the furnace cap after the samples were put inside the furnace. In a lot of prior studies [47,59,62], samples were exposed to high temperatures according to the ISO-834 fire curves [63]. In some studies, a constant heating rate of 10°C/min or 12°C/min was employed to achieve the elevated temperature of the specimen [62,64]. However, in this present investigation, a heating rate of 15°C/min was employed to increase the temperature of the furnace. Digital thermometers were used to record the temperature readings during exposure. Time *vs* temperature increase curve for elevated heating of about 200–600°C for the specimen recorded from thermocouples is shown in Figure 7(b). There was a time lag recorded for the temperature applied by a furnace and the observed temperature of the concrete specimen in the time *vs* temperature graph for the specimen. After attaining its ultimate temperature, the furnace's temperature was maintained for 2 h to ensure uniform distribution of temperature throughout the specimen such that the inside temperature of the specimen was at the same level as the furnace [62,65,66]. To prevent a fire from forming, the furnace was immediately shut off once the target heating of the specimen was reached. After shutting off the furnace, the samples were kept inside the furnace for

Table 5: Description of the specimens

Test type	Specimen geometry (mm)	No. of specimens
Compression	150 × 150 × 150	108 (18-control, 90-heated)
Split tensile	150 × 300	108 (18-control, 90-heated)
Flexural	100 × 100 × 500	108 (18-control, 90-heated)
Water permeability	150 × 150 × 150	108 (18-control, 90-heated)

(a) (b) (c)

Figure 6: Preparation of specimens (a) mixing of specimens, (b) casted specimens, (c) curing of samples.

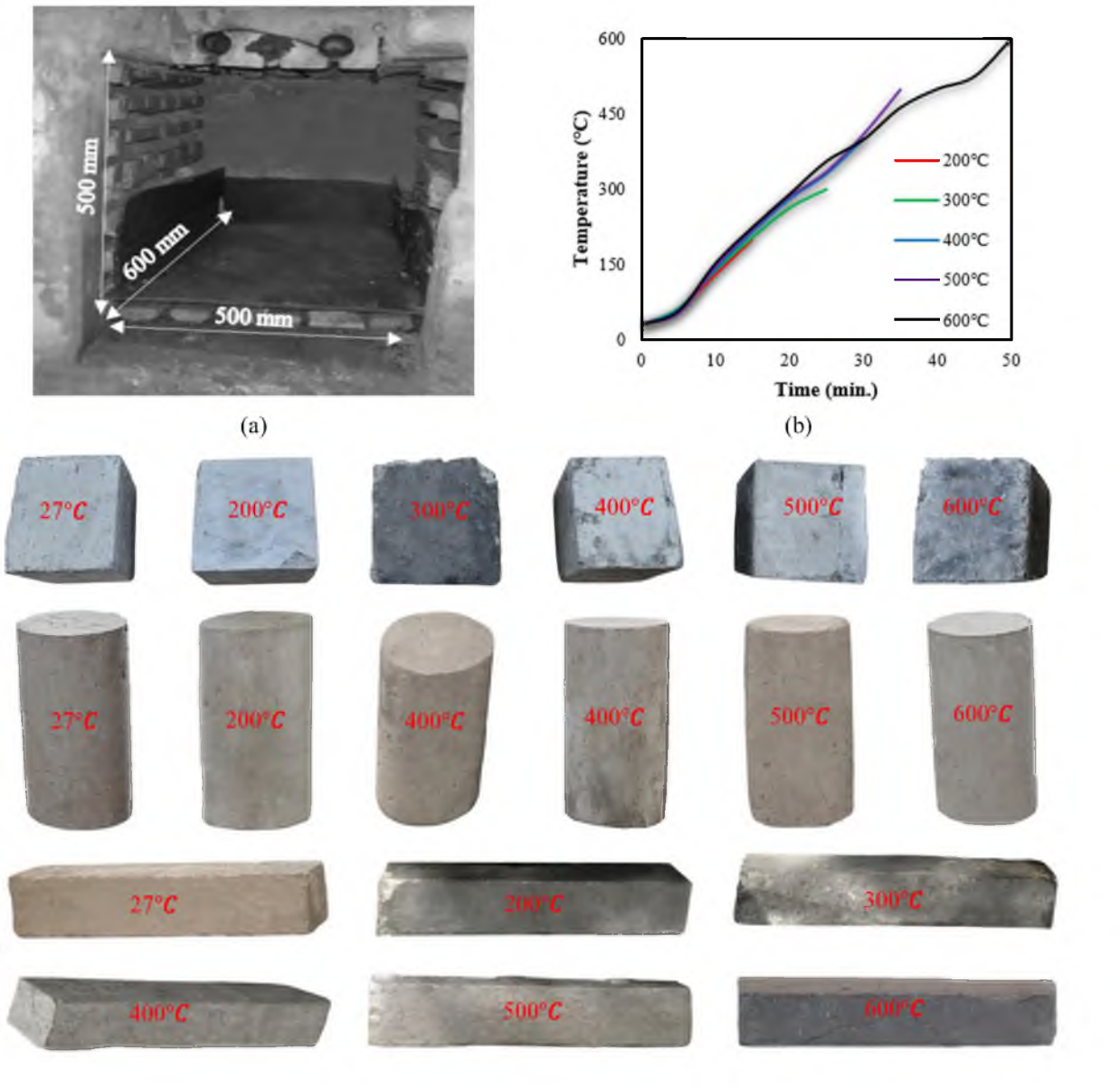

Figure 7: Heating procedure (a) electric furnace, (b) time *vs* temperature curve for specimen, (c) concrete specimens before and after exposure to raised temperature.

some time till the temperature of the specimens reduced to 100°C. Afterwards, the samples were placed to cool down in the air at room temperature.

2.4 Testing procedure

After heating and cooling down of the samples, the specimens were tested under different testing procedures as described in Figure 8. All the tests were conducted in the same manner for specimens exposed to elevated temperatures of about 200–600°C separately.

2.4.1 Mechanical properties

The mechanical properties were assessed by performing compression (on cubical specimens), split tensile (on cylindrical specimens), and flexural strength (on beam specimens) testing in accordance with the BIS 516:2021 [67]. The loading was raised at a constant rate till the specimens failed.

2.4.2 Ultrasonic pulse velocity (UPV) test

Before carrying out these mechanical strength tests, the weight loss and UPV tests were also accomplished for the cubical

concrete samples. The UPV experiments were executed in accordance with the BIS 516:2018 [68]. The UPV and mass loss of specimens can be determined by equations (1) and (2) as follows:

$$V = \frac{L}{T_L}, \tag{1}$$

$$M_L = \frac{M_1 - M_2}{M_1} \times 100. \tag{2}$$

2.4.3 Water permeability test

One set of cubical specimens was tested for water permeability test as per DIN 1045:1991 [69]. The test was conducted for 3 days with a water pressure of 0.5 MPa. Thereafter, the specimen was split into two parts from the centre with the aid of a compression testing machine. The depth of water penetrated inside the cube specimens was determined to represent the permeability of the concrete specimen.

2.4.4 Microstructure analysis

To assess the microstructure properties of concrete after exposure to high heat, SEM analysis was carried out by employing a Nova-Nano FE-SEM 450 machine on the specimen's debris obtained after the failure of specimens in compression testing. The residues were cleaned to remove any loose debris and contaminants by rinsing them in distilled water and then dried with the aid of a clean cloth by gentle patting. Then, the residues were placed in SEM holders and the surface of the residues was prepared by grinding or polishing to have a flat surface and transferred into the SEM chamber for SEM imaging.

3 Results and discussion

3.1 Specimen appearance

The experimental findings of the concrete samples with NBC and NFA indicated that concrete's colour changes when it is exposed to high temperatures. Concrete's colour changes depending on how much heat treatment is applied [70,71]. As the temperature rises from the ambient range, no notable alteration in the appearance of the samples was observed with no indication of cracks on the samples' surfaces. However, when the temperature of the samples hits

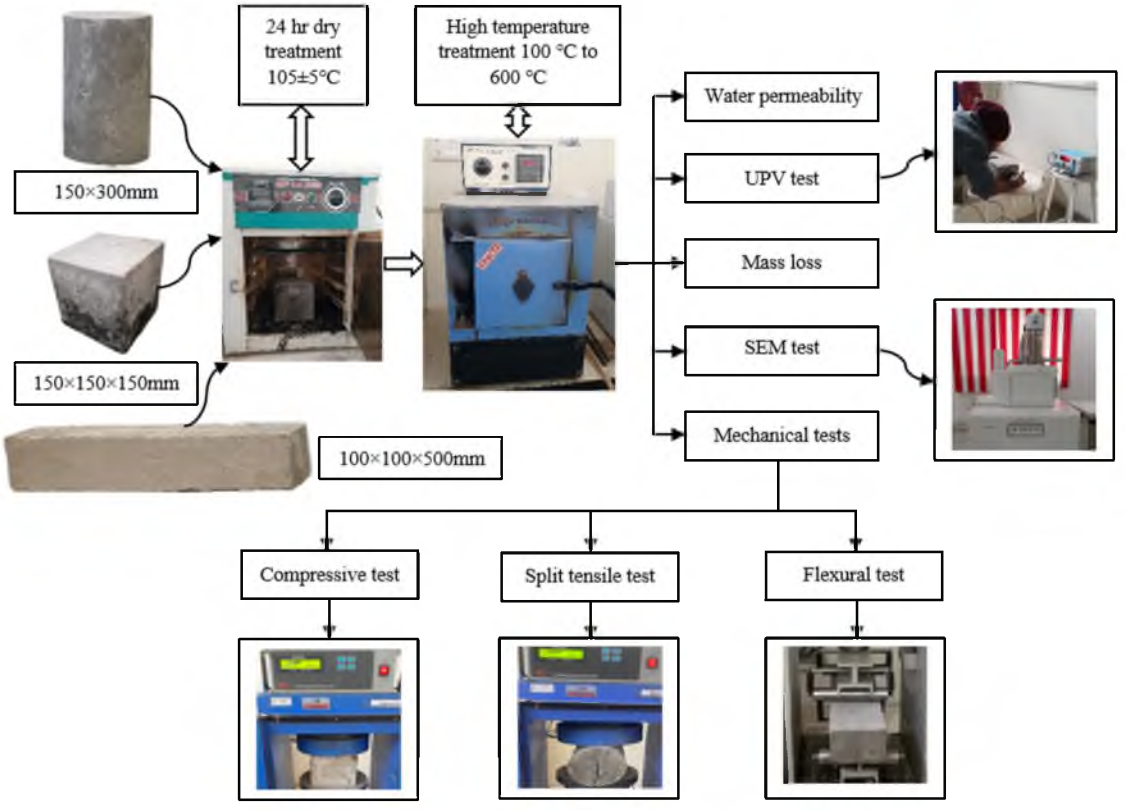

Figure 8: Testing of specimens after heat treatment.

200°C, the specimens become bright in colour probably due to the loss of free water [7]. A peak temperature of 300–400°C, however, produced darker colours in the specimens. Peak temperatures between 500 and 600°C caused the colour of the sample to turn from dark to light with grey stains on the surface owing to CO_2 combustion [8]. In accordance with the outcomes of the existing exploration, all types of concrete mix produced similar results.

Figure 9 illustrates that the visual appearance of specimens to which high temperatures were applied varies depending on the ratio of mix and temperatures applied. The appearance of the specimens slightly changes at temperatures of about 200–300°C. Although the surface of the specimens does not show any cracks at this point. The specimens' colours change from a light brown to a darker brown with a raise in the temperature to 400°C. In specimens at 500–600°C, small cracks can be observed and continuous long cracks can occur. Similar findings were observed by several researchers [72–74].

3.2 Compressive strength

The residual compression strength of concrete cubical samples with NBC and NFA after exposure to high temperature was determined *via* compression test. The findings of the compression test are presented in Figure 10 for all the specimens.

3.2.1 At ambient temperature

The compression resistance of concrete specimens was registered to be increased at lower proportions of NBC

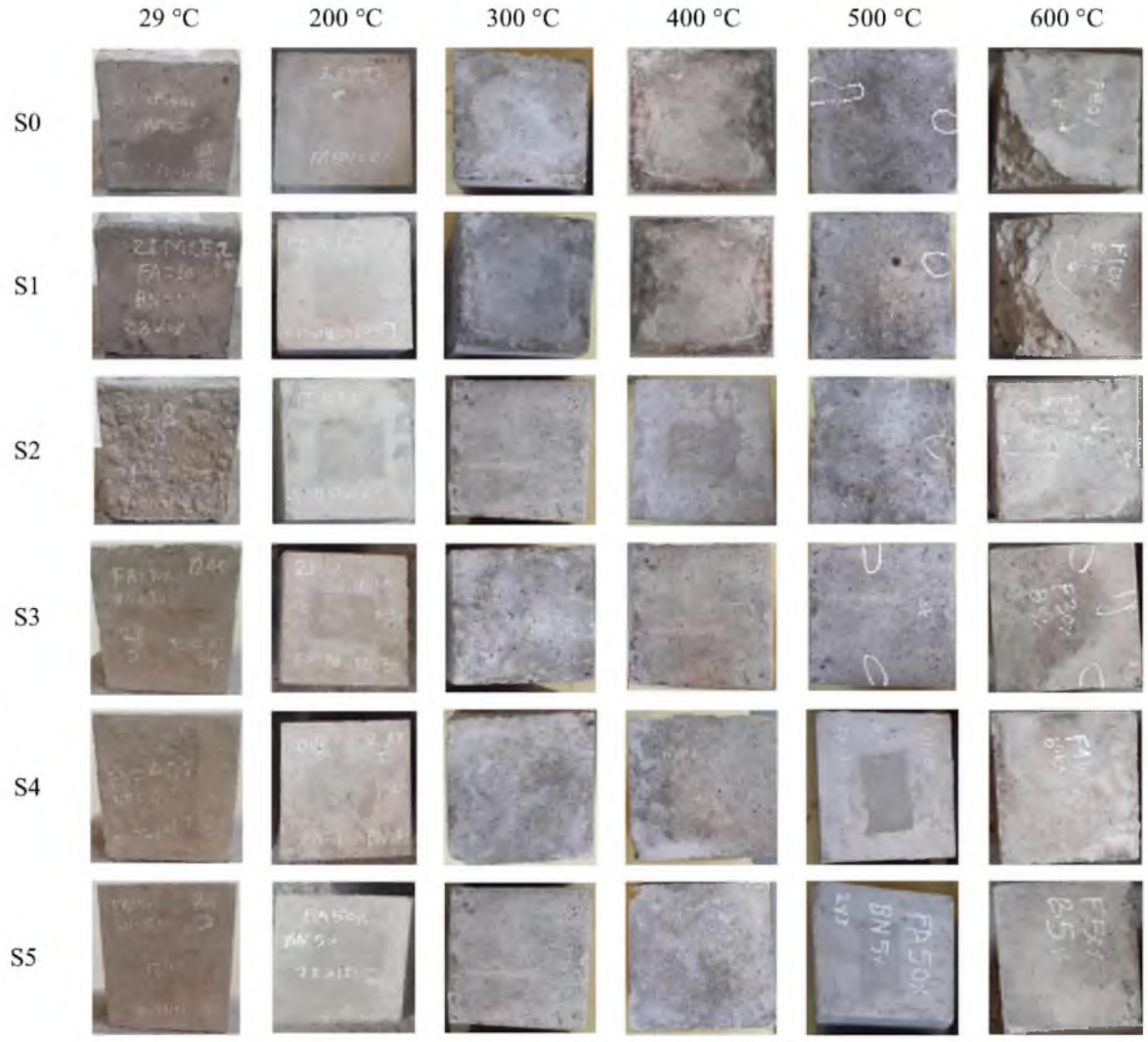

Figure 9: Appearance of specimens after heat application.

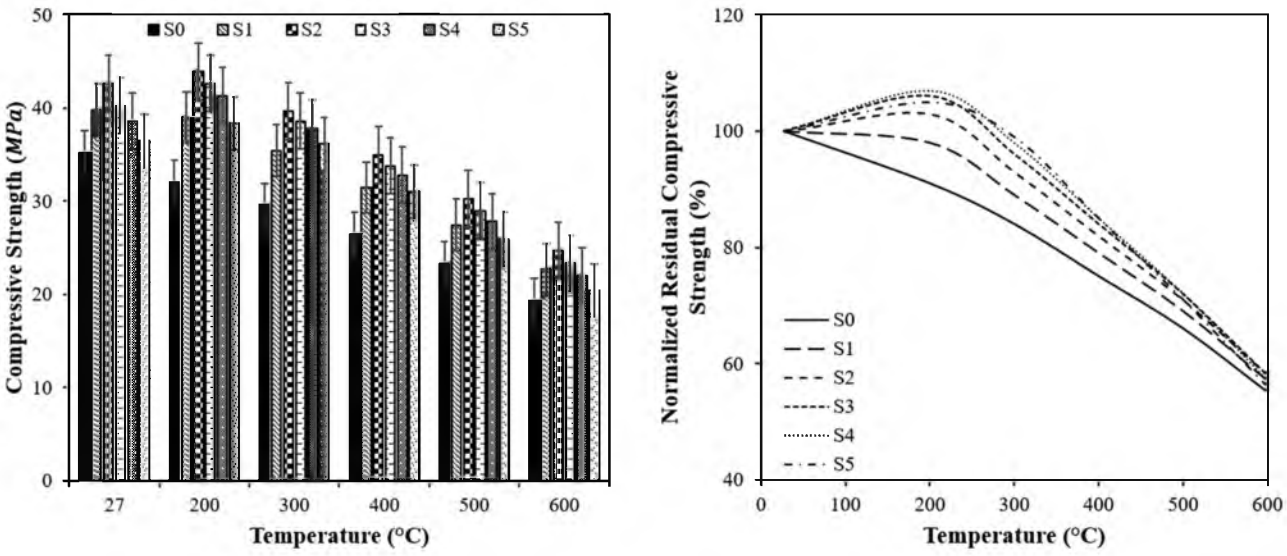

Figure 10: Compression test results (a) residual compressive strength, (b) normalized compressive strength.

and NFA. However, at higher proportions of these nanomaterials, the compression resistance was registered to be diminished [17]. The highest compression resistance at normal temperature was observed for S2, which increased the compressive strength by 21% as contrasted to the reference specimen.

3.2.2 At elevated temperature

Concrete's compression resistance at high temperatures depends on several factors, including additives, its strength at room temperature (29°C), and its heating rate [50]. As the temperature of specimens was increased from ambient temperature, the decrease in compression resistance was recorded. For control concrete specimens, the decline in the compression resistance occurred at 9, 16, 25, 34, and 45% as the temperature was raised to 200, 300, 400, 500, and 600°C, respectively. The loss of water from concrete when heated from 200 to 300°C causes hydrothermal changes [75]. Micro-cracking can occur when internal stresses are generated at 400°C [76]. The disintegration of $Ca(OH)_2$ occurs at temperatures greater than 400°C, leading to a further reduction in strength [77]. At about 500 and 600°C, calcium silicate hydrate (CSH) gel begins to decompose, resulting in a reduction in strength and stiffness [78]. A further loss of strength occurs when calcium carbonate ($CaCO_3$) decomposes between 500 and 600°C [75,79].

However, the specimen, with optimum compression strength at ambient temperature registered an increase in strength at a raised temperature of 200°C by 3%. Further rise in the exposure temperature led to the decrement of the compression strength of 7, 18, 29, and 42% for 300, 400, 500, and 600°C, respectively. Both regular concrete and concrete containing NBC and NFA experience small fractures owing to the breakdown of C–S–H gel and empty water capillaries. The reduction in compressive strength was found to be less in the case of concrete blended with NBC and NFA at elevated temperature in contrast to control specimens, which implies better performance of nano-modified concrete at elevated temperature.

3.3 Flexural strength

Based on the outcomes of a flexural strength test, the residual flexural strength of concrete prism/beam specimens with NBC and NFA after exposure to high temperatures was determined. The outcomes of the flexural strength experiment for each specimen are depicted in Figure 11. Behaviour similar to that seen in the compression resistance was recorded in the flexural strength test.

3.3.1 At ambient temperature

At lower proportions of NBC and NFA, the flexural strength of concrete samples was discovered to be increased, but at higher proportions of these nanomaterials, the flexural strength was recorded to be reduced [17]. The sample S2 had the greatest flexural strength at normal temperature, increasing the flexural strength by 10.11% in comparison to the control specimen.

3.3.2 At elevated temperature

Similar to the compressive strength, the flexural strength of concrete at raised temperatures is impacted by numerous variables, including additives, its strength at room temperature (27°C), and heating rate [50]. A decrease in flexural strength was seen as specimen temperatures were raised above ambient temperature. For control concrete specimens, the flexural strength decreased with temperature rise to 200, 300, 400, 500, and 600°C, respectively, by 2, 7, 12, 17, and 24%. Hydrothermal changes occur when concrete is heated from 200 to 300°C due to water loss [75]. The breakdown of CSH gel, drying of the cement mixture, and modification of aggregate crystal structure have been attributed to the decline in flexural strength. Additionally, due to the specimen's increased temperature, the bonding between the cement mix and the aggregates decreased, and tiny cracks and voids increased, which decreased the specimen's ability to resist bending [12,80,81].

However, for S2 specimens, a 3% gain in flexural strength was registered at the higher temperature of 200°C. Additionally, the flexural strength decreased by 2, 8, 14, and 22% while the temperature increased to 300, 400, 500, and 600°C, respectively. The drying of concrete and the breakdown of the bonding between the binder and the filler ingredient were the reasons for the decrease in flexural strength [82,83].

3.4 Split tensile strength

Through a split tensile capacity experiment, the residual split tensile strength of concrete cylinder specimens with NBC and NFA after exposure to high temperature was obtained. For all the specimens, the outcomes of the split tensile experiments are depicted in Figure 12.

3.4.1 At ambient temperature

Lower amounts of NBC and NFA were shown to increase the split tensile strength of concrete specimens. The tensile resistance, however, was recorded to diminish with larger ratios of these nanomaterials [17]. S2, which enhanced tensile strength by 10% in contrast to the reference specimen, had the maximum tensile resistance at standard normal temperature.

3.4.2 At elevated temperature

For control concrete samples, the tensile resistance decreased as the temperature increased to 200, 300, 400, 500, and 600°C, respectively, by 4, 8, 13, 19, and 26%. When heated to 200°C in relation to S2 samples, a 1% improvement in tensile resistance was noted. However, as the temperature was raised further to 300, 400, 500, and 600°C, respectively, there was a 4, 9, 16, and 24% decrease in the tensile strength. Several variables, including additives, concrete's strength at room temperature (29°C), and its heating rate, affect the material's tensile strength at high temperatures [50]. Due to the concrete's pore structure caused by the quick loss of moisture and its distinctive expansion of the cement mixture and other elements, the tensile strength of the concrete decreased [47,80]. Concrete loses water when heated from 200 to 300°C, which

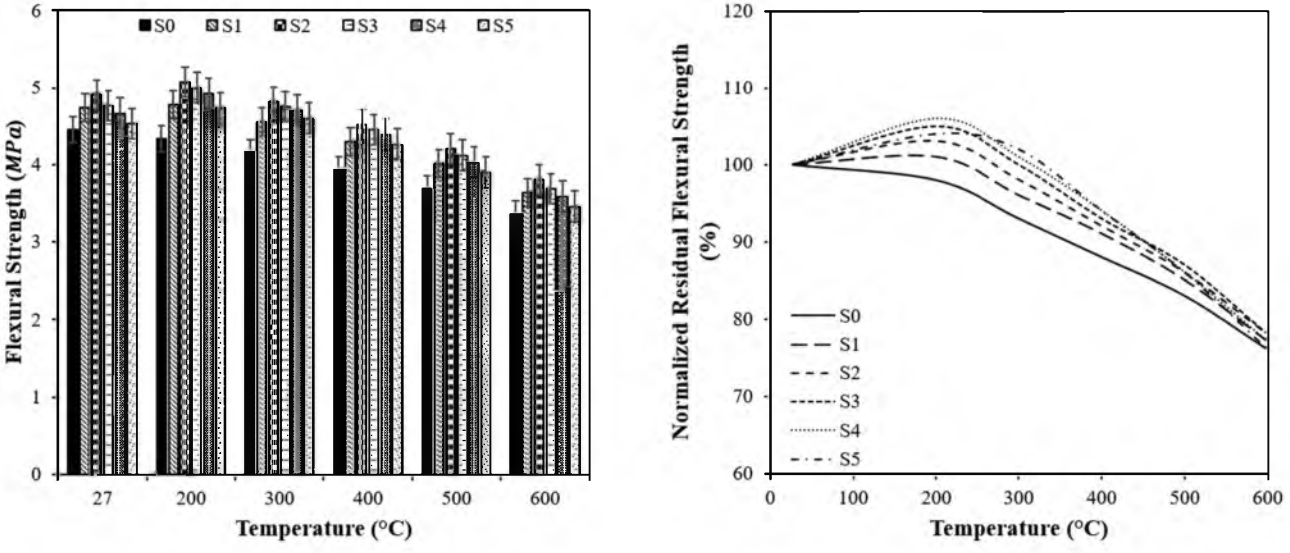

Figure 11: Flexural test results (a) residual flexural strength, (b) normalized flexural strength.

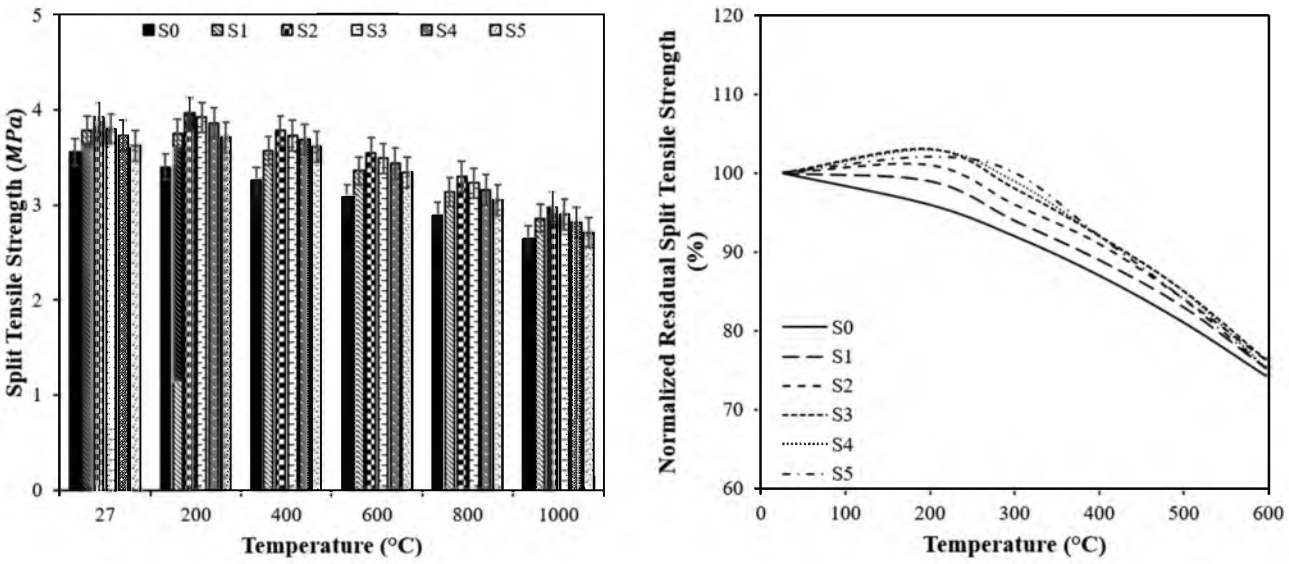

Figure 12: Split tensile strength test results (a) residual split tensile capacity, (b) normalized split tensile capacity.

results in hydrothermal alterations [75] and microcracking at 400°C due to internal stress development [76]. Calcium silicate hydrate (CSH) gel starts to break down between 500 and 600°C, which reduces its stiffness and strength [78]. When $CaCO_3$ breaks down between 500 and 600°C, strength is further reduced [75,79].

3.5 Water permeability

Concrete cubical specimens containing NBC and NFA were subjected to water penetration testing in accordance with DIN 1045:1991 [69]. Concrete cubes were fitted in the apparatus and water at 0.6 N/mm^2 of pressure was applied to the concrete surface by adding water to the water tank. The water permeability in terms of the depth of water penetrated inside the concrete specimens was determined. Based on measurements done for the specimens to which high temperature of 200, 300, 400, 500, and 600°C were applied, Figure 13 indicates an increase in water penetration depth as temperatures rise during the fire exposure. The test specimens exposed to fire are shown to have more penetration of water as the temperature rises. Higher temperatures result in more penetration of water, especially at 500 and 600°C.

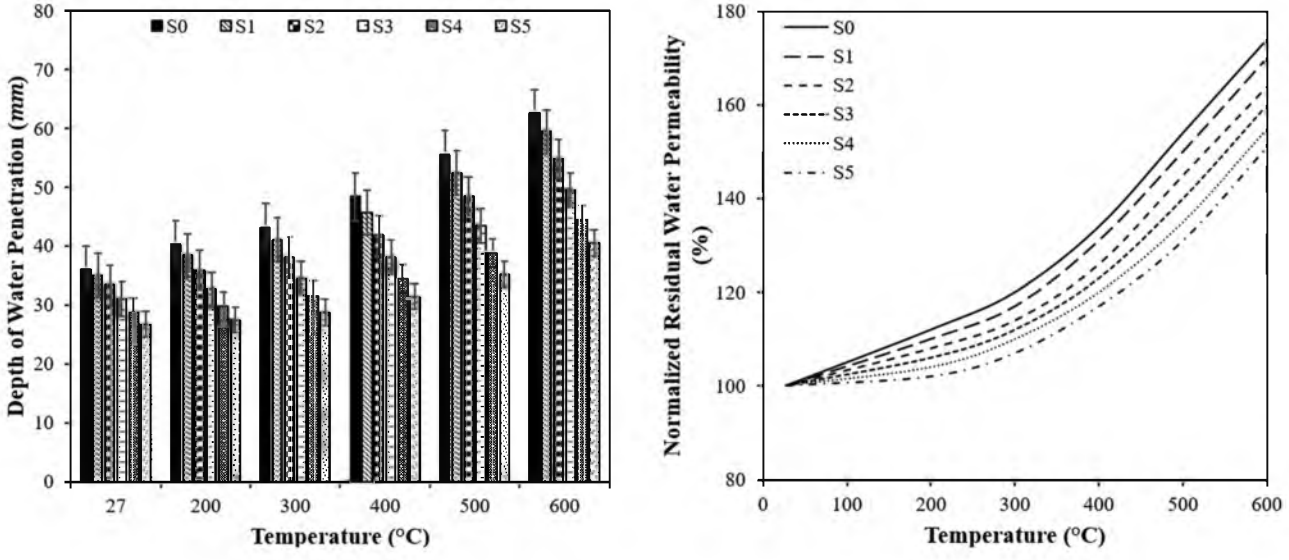

Figure 13: Water permeability test results (a) residual depth of water penetration, (b) normalized water permeability.

3.4.2 At ambient temperature

Nano bentonite and NFA replaced cement in the test results, resulting in a decrease in water penetration. Because NBC and NFA have smaller particle sizes than conventional cement, the binder phase is packed tightly. As a result, there is less porosity. Consequently, water is less likely to soak into the concrete due to this reduction in porosity [19,84]. The reduction in water penetration depth as 2.8, 7.2, 13.8, 20, and 25.5% was registered for specimens S1, S2, S3, S4, and S5 in comparison to control specimen.

3.4.3 At elevated temperature

For the control specimen, as the temperature was raised, increases in the penetration depth of water as 12, 20, 34, 54, and 74% were recorded in case of temperature exposure to 200, 300, 400, 500, and 600°C, respectively. The specimen S2, which resulted in optimum mechanical resistance outcomes, showed an increase in the depth of water penetration by 8, 14, 26, 45, and 64% after temperature exposure of 200, 300, 400, 500, and 600°C, respectively. However, maximum control on the water permeability was reflected by the specimen S5 with 2, 7, 17, 31, and 51% increases in the water permeability when high temperatures of 200, 300, 400, 500, and 600°C were applied to the specimens, respectively. The rapid evaporation of moisture increases, resulting in the porous concrete structure [85]. The micro-cracks change to macro-cracks owing to the distinctive thermal expansion of binder and filler materials in concrete, leading to higher water permeability of concrete specimens [86,87].

3.5 Mass loss

Mass loss of concrete makes a significant contribution to its durability evaluation. The mass of specimens with or without the utilization of NBC and NFA at normal temperature and after application of high temperature is presented in Figure 14.

3.5.1 At ambient temperature

It was demonstrated that the use of such nanomaterials increases the mass of specimens due to more dense structure. However, the mass of specimens was observed to decrease with an increment in the heating temperature [31,88]. The increment of 0.6, 1.1, 1.4, 1.6, and 1.9% in the weight of the concrete samples were observed for S1, S2, S3, S4, and S5 samples in contrast to reference samples.

3.5.2 At elevated temperature

As the temperature increased from room temperature to 200, 300, 400, 500, and 600°C, the loss in the mass of the specimens was determined as 2, 4, 7, 10, and 13%, respectively, for the control specimens. Similarly, for S2

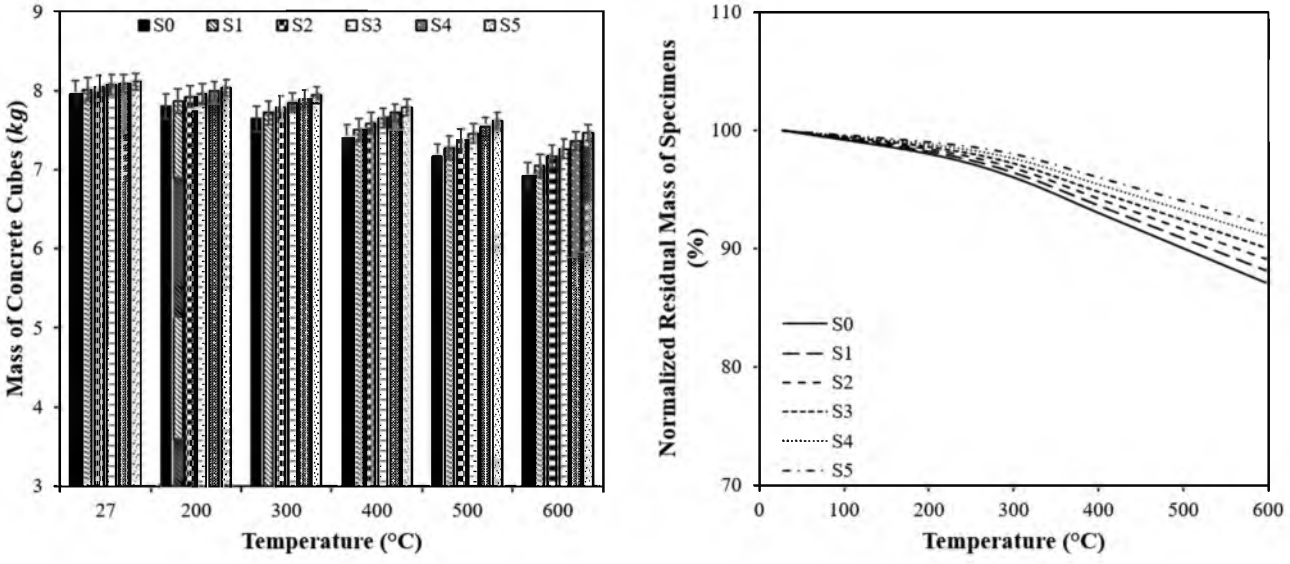

Figure 14: Mass of specimens (a) residual mass, (b) normalized mass.

specimens, the mass loss was obtained as 1.6, 3.2, 5.8, 8.4, and 11% after exposure to high temperature of about 200, 300, 400, 500, and 600°C, respectively. Further, the sample S5 showed a greater reduction in the mass loss at 1, 2, 4, 6, and 8% while the temperature of exposure increased from standard normal temperature to 200, 300, 400, 500, and 600°C, respectively. The reduction in mass at greater temperatures could be owing to the expulsion of chemically bound water, which is a component of cement hydration compounds and is extremely hard to disperse. This water leaks out of the concrete as the hydration compounds break down due to heating [52,83,89–91]. Concrete mass decreased as a consequence of the CSH gel's dissolution, varied temperature stresses within the material, and the quick drying of the concrete. The weight of the concrete decreased after imposing high temperatures because the porousness of the concrete specimen increased and the bond between the cement mix and other elements was weakened [59,92].

3.6 UPV

An UPV experiment can be employed to evaluate the internal deterioration generated by raised temperatures in a concrete specimen. The UPV test outcomes for the specimens with and without NBC and NFA at elevated temperature exposure are presented in Figure 15.

3.6.1 At ambient temperature

The UPV values were found to be increased due to the substitution of NBC and NFA. The UPV values were increase by 4, 7, 9.5, 11.2, and 12.7% for the specimens S1, S2, S3, S4, and S5, respectively, in contrast to control specimen.

3.6.2 At elevated temperature

In Figure 15, when the temperature of the specimens was increased, the UPV decreased. For the reference specimen, the decrease in the UPV outcomes was registered as 9, 17, 28, 37, and 44% for the temperature exposure of 200, 300, 400, 500, and 600°C, respectively. Increasing temperature results in more internal damage of the test specimen, and reflected in an increase in the degree of damage [93]. The UPV outcomes decline significantly from 400 to 600°C owing to capillary water deprivation and ettringite drying. Further, for S2 specimens, reductions in the UPV results were obtained as 8, 16, 23, 31, and 39%. Similarly for the specimen, S5, the lowest reduction in UPV findings was 6, 11.9. 18.1, 24.1, and 30% was observed when high temperature of 200, 300, 400, 500, and 600°C was applied, respectively. Due to the expansion of fractures, weakening of the bonding among the aggregates, dissolution of the CSH gel, and quick loss of water, which gave rise to the generation of concrete's porosity and the emergence of significant empty spaces, the pulse velocity decreased [12,51,87,94].

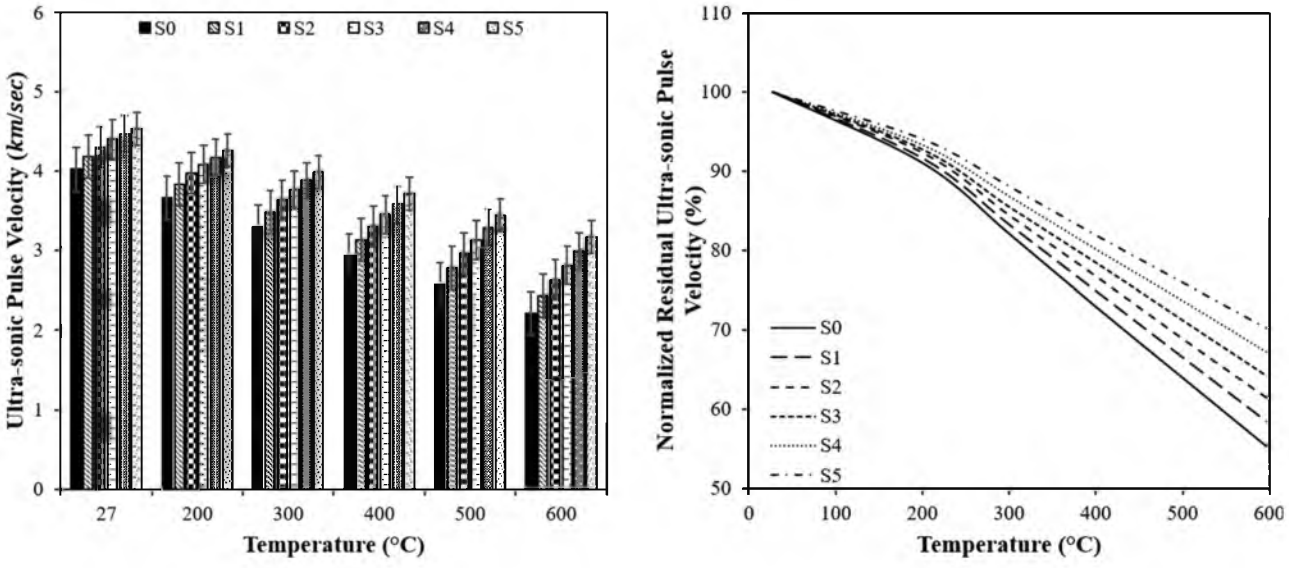

Figure 15: UPV results (a) UPV values of specimens, (b) normalized UPV values.

3.7 SEM

The thermal decomposition of concrete's constituent materials causes it to undergo microstructural changes at high temperatures. The extent and nature of these changes depend on the temperature and duration of exposure. SEM analysis can characterize the microstructure of concrete after high-temperature treatment. Using SEM images, the morphology, size, and distribution of concrete components can be observed. A high-temperature analysis can also reveal the extent to which the microstructure has been damaged or degraded. Figure 16 illustrates the SEM

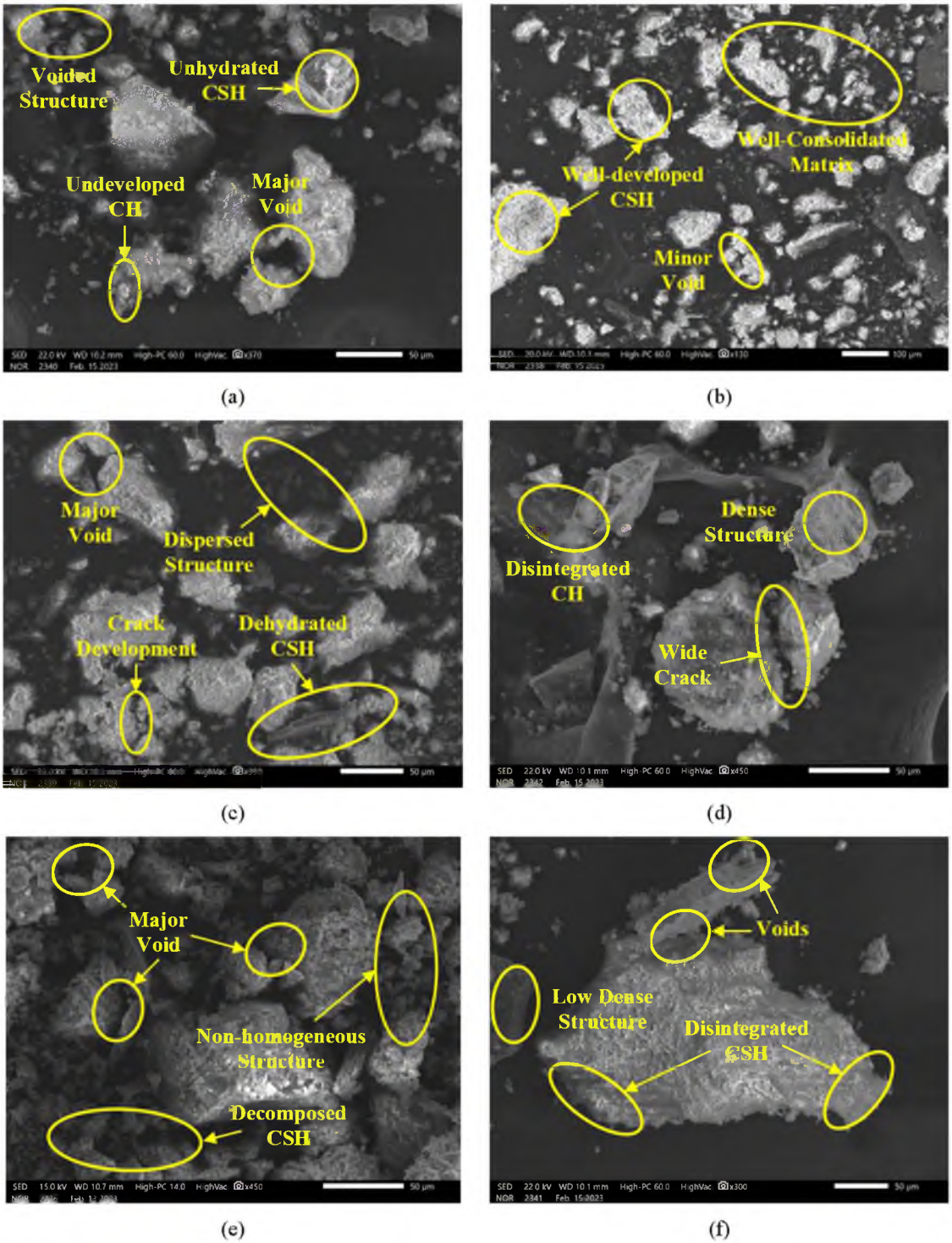

Figure 16: SEM images for concrete specimen (a) S0 (27°C), (b) S2 (27°C), (c) S0 (200°C), (d) S2 (200°C), (e) S0 (600°C), (f) S2 (600°C).

images for the control concrete specimen (NC) and optimum strength concrete specimen (S2). The SEM images at ambient temperature, at the onset of elevated temperature (200°C) and at the peak temperature of 600°C was compared to get an idea of the behaviour of concrete specimens at lower and higher temperature range.

The SEM results of S2 are collected because they resulted in the optimum mechanical strength increase of the control specimen at almost all the temperature ranges. A concrete specimen at a normal temperature of 27°C has a tightly combined structure, is compact, and contains dense phases in both cases of concrete specimens. However, in the case of the control specimen at this stage, some undeveloped CSH and some void can be observed. Furthermore, there is a large amount of crystal water and gel present at this stage in the case of the S2 specimen with minor voids only and a well-consolidated matrix. When the sample is heated to 200°C, the control specimens are shown to have some major voids and some crack development. Water vaporizes and evaporates from internal free space as well as capillary spaces. C–S–H gel also loses adsorbed water through cement hydration, resulting in cement dehydration [70,95] and a dispersed structure was observed. In the case of S2 concrete specimen shows still a dense structure with minor disintegration of CH and some crack development at a temperature of 200°C. The concrete surface appears porous at temperatures of 600°C because a great deal of water is lost. Additionally, the concrete structure is destroyed, resulting in a non-homogeneous structure for the control specimen. It appears that the control specimens appear white and cracks appear on their surfaces at this temperature. As a result of further decomposition and loosening, the specimens show major voids at 600°C [92,96]. The $Ca(OH)_2$ hydration byproduct turned dehydrated as a consequence of a spike in temperature since the water that was soaked by the CSH paste vaporized resulting in the disintegration of CSH paste in the case of the S2 specimen at a temperature of 600°C. The low-dense structure appeared in the SEM images with some voids at temperatures of 600°C along with CSH paste breakdown which led to a loss in mechanical strength [62,65]. Nonetheless, better post-fire performance was observed for the concrete specimens incorporating the NBC and NFA with fewer cracks and void development.

4 Conclusion

In the present investigation, the impact of NBC and NFA on the mechanical and durability characteristics of concrete specimens implemented at elevated temperatures was determined through an experimental program. Post the study, the salient points that were extracted from the study are listed below:

- The mechanical strengths of the concrete samples recorded improved with the substitution of nano bentonite and NFA at room and elevated temperatures. The optimum content of NBC and NFA was determined to be 2%, and 20% at which better mechanical properties of the concrete was observed. However, further substitution of NBC and NFA beyond this limit gave rise to a decrease in the mechanical resistance.
- At the elevated temperature, the mechanical strengths were observed to decrease. However, the specimen having 2% NBC and 20% NFA showed the highest residual mechanical strength as compared with other samples.
- The water permeability of concrete specimens with NBC and NFA decreased due to the condensed and close-packed structure of such concrete specimens. Also, the loss of mass was less in the case of specimens with NBC and NFA. Due to the increase in mass, and less porous, compact, and dense structure, the UPV in the concrete samples also increased. However, as the temperature increased, decrease in the mass and UPV outcomes with a rise in permeability can be seen.
- The substitution of NBC and NFA increases the compactness of concrete by filling the pore of concrete resulting in less crack formation at the lower temperatures of the range 200°C. However, as the temperature further increases, development of micro and some major fissures might be reflected on the concrete surface. The SEM analysis of the concrete specimen with optimum content of NBC and NFA also indicated that the microstructure of concrete gets improved owing to the addition of these nanomaterials. Owing to the disintegration of CSH gel and increase in the porosity, wide cracks and irregular structures were observed at temperature exposures of more than 400°C.

It was demonstrated in the above study that the use of NBC (2%) and NFA (20%) in the concrete can lead to an improvement in residual characteristics of concrete post the application of elevated temperatures up to 200°C. However, further increases in the temperature can result in the degradation of the residual characteristics, yet it showed better mechanical properties in contrast with the specimens without the use of such nanomaterials.

5 Future scope

Following are the future perspective of the study:

- **Long-term durability evaluation:** Further research into the behaviour of the concrete composed of NBC and NFA

under high-temperature exposure might be done by carrying out experiments such as freeze–thaw cycles, alkali-silica reaction, sulphate attack, carbonation resistance, *etc.*

- **Effect of curing methods:** It is possible to investigate the effects of several curing processes, such as water curing, steam curing, or accelerated curing, on the characteristics of concrete prepared with NBC and NFA and heated to a high temperature.
- **Behaviour under various temperature regimes:** The research may be expanded to examine the qualities of concrete containing NBC and NFA subjected to high-temperature regimes by replicating various fire exposure scenarios at varied temperatures and exposure times.
- **Environmental considerations:** By examining energy consumption, carbon footprint, and life cycle assessments, research on the environmental impact and sustainability aspects of using NBC and NFA in concrete at elevated temperatures can be done. This will help researchers to comprehend the overall environmental advantages of these materials.

Funding information: The authors state no funding involved.

Author contributions: All authors have accepted responsibility for the entire content of this manuscript and approved its submission.

Conflict of interest: The authors state no conflict of interest.

References

[1] Mohamadien HA. The Effect of marble powder and silica fume as partial replacement for cement on mortar. Int J Civ Struct Eng. 2012;3:418–28. doi: 10.6088/ijcser.201203013039.

[2] Demirel B. The effect of the using waste marble dust as fine sand on the mechanical properties of the concrete. Int J Phys Sci. 2010;5:1372–80.

[3] Acchar W, Vieira FA, Hotza D. Effect of marble and granite sludge in clay materials. Mater Sci Eng A. 2006;419:306–9. doi: 10.1016/j.msea.2006.01.021.

[4] Koksal F, Kocabeyoglu ET, Gencel O, Benli A. The effects of high temperature and cooling regimes on the mechanical and durability properties of basalt fiber reinforced mortars with silica fume. Cem Concr Compos. 2021;121:104107. doi: 10.1016/j.cemconcomp.2021.104107.

[5] Hager I. Behaviour of cement concrete at high temperature. Bull Pol Acad Sci Tech Sci. 2013;61:145–54. doi: 10.2478/bpasts-2013-0013.

[6] Arslan F, Benli A, Karatas M. Effect of high temperature on the performance of self-compacting mortars produced with calcined kaolin and metakaolin. Constr Build Mater. 2020;256:119497. doi: 10.1016/j.conbuildmat.2020.119497.

[7] Pachta V, Tsardaka EC, Stefanidou M. The role of flame retardants in cement mortars exposed at elevated temperatures. Constr Build Mater. 2021;273:122029. doi: 10.1016/j.conbuildmat.2020.122029.

[8] Pachta V, Anastasiou EK. Utilization of industrial byproducts for enhancing the properties of cement mortars at elevated temperatures. Sustainability (Switz). 2021;13:12104. doi: 10.3390/su132112104.

[9] Shihada S. Effect of polypropylene fibers on concrete fire resistance. J Civ Eng Manag. 2011;17:259–64. doi: 10.3846/13923730.2011.574454.

[10] Dong H, Cao W, Bian J, Zhang J. The fire resistance performance of recycled aggregate concrete columns with different concrete compressive strengths. Materials. 2014;7:7843–60. doi: 10.3390/ma7127843.

[11] Chen B, Li C, Chen L. Experimental study of mechanical properties of normal-strength concrete exposed to high temperatures at an early age. Fire Saf J. 2009;44:997–1002. doi: 10.1016/j.firesaf.2009.06.007.

[12] Kiran T, Yadav SK, Anand N, Mathews ME, Andrushia D, Lubloy E, et al. Performance evaluation of lightweight insulating plaster for enhancing the fire endurance of high strength structural concrete. J Build Eng. 2022;57:104902. doi: 10.1016/j.jobe.2022.104902.

[13] Tanyildizi H, Coskun A. The effect of high temperature on compressive strength and splitting tensile strength of structural lightweight concrete containing fly ash. Constr Build Mater. 2008;22:2269–75. doi: 10.1016/j.conbuildmat.2007.07.033.

[14] Kiran T, Mathews ME, Anand N, Alengaram UJ, Andrushia AD. Influence of mineral admixtures on the residual mechanical properties and durability characteristics of self-compacting concrete subjected to high temperature. Aust J Civ Eng. 2022;20:244–60. doi: 10.1080/14488353.2021.1953682.

[15] Xu Y, Wong YL, Poon CS, Anson M. Impact of high temperature on PFA concrete. Cem Concr Res. 2001;31:1065–73.

[16] Marzouk HM, Hussein A. Properties of high-strength concrete at low temperatures. ACI Mater J. 1990;87:167–71.

[17] Ahmad S, Barbhuiya SA, Elahi A, Iqbal J. Effect of Pakistani bentonite on properties of mortar and concrete. Clay Min. 2011;46:85–92. doi: 10.1180/claymin.2011.046.1.85.

[18] Vamsi G, Reddy K, Rao VR, Achyutha M, Reddy K, Rao R. Experimental investigation of strength parameters of cement and concrete by partial replacement of cement with Indian calcium bentonite. Int J Civ Eng Technol. 2017;8:512–8.

[19] Adeboje AO, Kupolati WK, Sadiku ER, Ndambuki JM, Kambole C. Experimental investigation of modified bentonite clay-crumb rubber concrete. Constr Build Mater. 2020;233:117187. doi: 10.1016/j.conbuildmat.2019.117187.

[20] Uddin F. Clays, nanoclays, and montmorillonite minerals. Metall Mater Trans A Phys Metall Mater Sci. 2008;39:2804–14. doi: 10.1007/s11661-008-9603-5.

[21] Uddin MK. A review on the adsorption of heavy metals by clay minerals, with special focus on the past decade. Chem Eng J. 2017;308:438–62. doi: 10.1016/j.cej.2016.09.029.

[22] Alobaidi YM, Hilal NN, Faraj RH. An experimental investigation on the nano-fly ash preparation and its effects on the performance of self-compacting concrete at normal and elevated temperatures. Nanotechnol Environ Eng. 2021;6:1–13. doi: 10.1007/s41204-020-00098-6.

[23] Jha P, Sachan AK, Singh RP. Utilization of stone dust as an effective alternative for sand replacement in concrete. 3rd International Conference on Innovative Technologies for Clean and Sustainable Development: ITCSD 2020. RILEM Bookseries, vol. 29, Cham: Springer International Publishing; 2021. p. 513–26. doi: 10.1007/978-3-030-51485-3_34.

[24] Jha P, Sachan AK, Singh RP. Bagasse ash (ScBa) and its utilization in concrete as pozzolanic material: A review. Lecture notes in civil engineering, Vol. 143 LNCE, Singapore: Springer Science and Business Media Deutschland GmbH; 2021. p. 471–80. doi: 10.1007/978-981-33-6969-6_41.

[25] Nagendra V, Prasanna Kumar SM, Venkata Ramana N. GGBS and Nano silica (NS) effect on concrete. Int J Civ Eng Technol. 2016;7:477–84.

[26] Saini G, Vattipalli U. Assessing properties of alkali activated GGBS based self-compacting geopolymer concrete using nano-silica. Case Stud Constr Mater. 2020;12:e00352. doi: 10.1016/j.cscm.2020.e00352.

[27] Chiranjeevi K, Vijayalakshmi MM, Praveenkumar TR. Investigation of fly ash and rice husk ash-based geopolymer concrete using nano particles. Appl Nanosci (Switz). 2021;13:839–42. doi: 10.1007/s13204-021-01916-2.

[28] Qureshi LA, Ali B, Ali A. Combined effects of supplementary cementitious materials (silica fume, GGBS, fly ash and rice husk ash) and steel fiber on the hardened properties of recycled aggregate concrete. Constr Build Mater. 2020;263:120636. doi: 10.1016/j.conbuildmat.2020.120636.

[29] Behnood A, Ziari H. Effects of silica fume addition and water to cement ratio on the properties of high-strength concrete after exposure to high temperatures. Cem Concr Compos. 2008;30:106–12. doi: 10.1016/j.cemconcomp.2007.06.003.

[30] Wang W, Lu C, Li Y, Li Q. An investigation on thermal conductivity of fly ash concrete after elevated temperature exposure. Constr Build Mater. 2017;148:148–54. doi: 10.1016/j.conbuildmat.2017.05.068.

[31] Siddique R, Kaur D. Properties of concrete containing ground granulated blast furnace slag (GGBFS) at elevated temperatures. J Adv Res. 2012;3:45–51. doi: 10.1016/j.jare.2011.03.004.

[32] Lau A, Anson M. Effect of high temperatures on high performance steel fibre reinforced concrete. Cem Concr Res. 2006;36:1698–707. doi: 10.1016/j.cemconres.2006.03.024.

[33] Baloch WL, Khushnood RA, Memon SA, Ahmed W, Ahmad S. Effect of elevated temperatures on mechanical performance of normal and lightweight concretes reinforced with carbon nanotubes. Fire Technol. 2018;54:1331–67. doi: 10.1007/s10694-018-0733-z.

[34] Ahmed HU, Mohammed AS, Faraj RH, Qaidi SMA, Mohammed AA. Compressive strength of geopolymer concrete modified with nano-silica: Experimental and modeling investigations. Case Stud Constr Mater. 2022;16:e01036. doi: 10.1016/j.cscm.2022.e01036.

[35] Singh H, Tiwary AK, Eldin SM, Ilyas RA. Behavior of stiffened concrete-filled steel tube columns infilled with nanomaterial-based concrete subjected to axial compression. J Mater Res Technol. 2023;24:9580–93. doi: 10.1016/j.jmrt.2023.05.135.

[36] Murad YZ, Aljaafreh AJ, AlMashaqbeh A, Alfaouri QT. Cyclic Behaviour of Heat-Damaged Beam–Column Joints Modified with Nano-Silica, Nano-Titanium, and Nano-Alumina. Sustainability (Switz). 2022;14:10916. doi: 10.3390/su141710916.

[37] Atiq Orakzai M. Hybrid effect of nano-alumina and nano-titanium dioxide on Mechanical properties of concrete. Case Stud Constr Mater. 2021;14:e00483. doi: 10.1016/j.cscm.2020.e00483.

[38] Wang L, Zhang P, Golewski G, Guan J. Editorial: Fabrication and properties of concrete containing industrial waste. Front Mater. 2023;10:1169715. doi: 10.3389/fmats.2023.1169715.

[39] Jha P, Sachan AK, Singh RP. An overview: Supplementary cementitious materials. Advances in construction materials and sustainable environment: Select Proceedings of ICCME 2020. Singapore: Springer Singapore; 2022. p. 53–63.

[40] Golewski GL. Mechanical properties and brittleness of concrete made by combined fly ash, silica fume and nanosilica with ordinary Portland cement. AIMS Mater Sci. 2023;10:390–404. doi: 10.3934/matersci.2023021.

[41] Ramanathan V, Feng Y. Air pollution, greenhouse gases and climate change: Global and regional perspectives. Atmos Environ. 2009;43:37–50. doi: 10.1016/j.atmosenv.2008.09.063.

[42] Asim W, Hussain M, Kadhim NR, Abdulrasool AT, Alhabeeb SA, Mohammed SS. Influence of using nano-clay hydrophilic bentonite on mechanical properties of concrete. J Posit Sch Psychol. 2022;2022:6583–7.

[43] Mirza J, Riaz M, Naseer A, Rehman F, Khan AN, Ali Q. Pakistani bentonite in mortars and concrete as low cost construction material. Appl Clay Sci. 2009;45:220–6. doi: 10.1016/j.clay.2009.06.011.

[44] Sujay HM, Nair NA, Sudarsana Rao H, Sairam V. Experimental study on durability characteristics of composite fiber reinforced high-performance concrete incorporating nanosilica and ultra fine fly ash. Constr Build Mater. 2020;262:120738. doi: 10.1016/j.conbuildmat.2020.120738.

[45] IS 8112: 2013. Ordinary Portland Cement; 43 Grade-Specification. Bureau of Indian Standards, New Delhi, India, 2013. n.d.

[46] IS 383-2016. Coarse and Fine Aggregate for Concrete – Specification. Bureau of Indian Standards, New Delhi-110002, Indian, 2016. n.d.

[47] Tiwary AK, Singh S, Kumar R, Chohan JS, Sharma S, Singh J, et al. Effects of elevated temperature on the residual behavior of concrete containing marble dust and foundry sand. Materials. 2022;15:3632. doi: 10.3390/ma15103632.

[48] Singh G, Tiwary AK, Singh S, Kumar R, Chohan JS, Sharma S, et al. Incorporation of silica fumes and waste glass powder on concrete properties containing crumb rubber as a partial replacement of fine aggregates. Sustainability (Switz). 2022;14:14453. doi: 10.3390/su142114453.

[49] Junaid Akbar E, Alam B, Ashraf M, Afzal S, Akbar J, Ahmad A, et al. Evaluating the effect of bentonite on strength and durability of high performance concrete. Int J Adv Struct Geotech Eng. 2013;2:2319–5347.

[50] Farhan Mushtaq S, Ali A, Khushnood RA, Tufail RF, Majdi A, Nawaz A, et al. Effect of bentonite as partial replacement of cement on residual properties of concrete exposed to elevated temperatures. Sustainability (Switz). 2022;14:11580. doi: 10.3390/su141811580.

[51] Hager I, Sitarz M, Mróz K. Fly-ash based geopolymer mortar for high-temperature application – Effect of slag addition. J Clean Prod. 2021;316:128168. doi: 10.1016/j.jclepro.2021.128168.

[52] Abdelmelek N, Lubloy E. Flexural strength of silica fume, fly ash, and metakaolin of hardened cement paste after exposure to elevated temperatures. J Therm Anal Calorim. 2022;147:7159–69. doi: 10.1007/s10973-021-11035-3.

[53] IS 10262: 2019. Concrete Mix Proportioning – Guidelines. Bureau of Indian Standards, New Delhi, India, 2019. n.d.

[54] Garg R, Garg R, Eddy NO, Khan MA, Khan AH, Alomayri T, et al. Mechanical strength and durability analysis of mortars prepared

with fly ash and nano-metakaolin. Case Stud Constr Mater. 2023;18:e01796. doi: 10.1016/j.cscm.2022.e01796.
[55] Carmichael MJ, Arulraj GP, Meyyappan PL. Effect of partial replacement of cement with nano fly ash on permeable concrete: A strength study. Mater Today Proc. 2020;43:2109–16. Elsevier Ltd. doi: 10.1016/j.matpr.2020.11.891.
[56] Arulraj GP, Carmichael MJ. Effect of Nano Flyash on Strength of Concrete. Int J Civ Struct Eng. 2011;2:475–82.
[57] Dahish HA, Almutairi AD. Effect of elevated temperatures on the compressive strength of nano-silica and nano-clay modified concretes using response surface methodology. Case Stud Constr Mater. 2023;18:e02032. doi: 10.1016/j.cscm.2023.e02032.
[58] Jaafar MFM, Mohd Saman H, Muhd Sidek MN, Muthusamy K, Ismail N. Performance of nano metaclay on chloride diffusion for ultra-high performance concrete. IOP Conference Series: Earth and Environmental Science. Vol. 682. IOP Publishing Ltd; 2021. doi: 10.1088/1755-1315/682/1/012002.
[59] Kanagaraj B, Anand N, Andrushia AD, Lubloy E. Investigation on engineering properties and micro-structure characteristics of low strength and high strength geopolymer composites subjected to standard temperature exposure. Case Stud Constr Mater. 2022;17:e01608. doi: 10.1016/j.cscm.2022.e01608.
[60] Jha P, Sachan AK, Singh RP. Investigation on the durability of concrete with partial replacement of cement by bagasse ash (BAH) and sand by stone dust (SDT). Mater Today Proc. 2020;43:237–43. doi: 10.1016/j.matpr.2020.11.652. Elsevier Ltd.
[61] Kumar R, Singh S, Singh LP. Studies on enhanced thermally stable high strength concrete incorporating silica nanoparticles. Constr Build Mater. 2017;153:506–13. doi: 10.1016/j.conbuildmat.2017.07.057.
[62] Shumuye ED, Zhao J, Wang Z. Effect of fire exposure on physico-mechanical and microstructural properties of concrete containing high volume slag cement. Constr Build Mater. 2019;213:447–58. doi: 10.1016/j.conbuildmat.2019.04.079.
[63] ISO 834-11:2014. Fire resistance tests-Elements of building construction-Part 11: Specific requirements for the assessment of fire protection to structural steel elements. International Organization for Standardization, Geneva, Switzerland, 2014. n.d.
[64] Wang Y, Liu F, Xu L, Zhao H. Effect of elevated temperatures and cooling methods on strength of concrete made with coarse and fine recycled concrete aggregates. Constr Build Mater. 2019;210:540–7. doi: 10.1016/j.conbuildmat.2019.03.215.
[65] Tung TM, Babalola OE, Le D-H. Experimental investigation of the performance of ground granulated blast furnace slag blended recycled aggregate concrete exposed to elevated temperatures. Clean Waste Syst. 2023;4:100069. doi: 10.1016/j.clwas.2022.100069.
[66] Varona FB, Baeza-Brotons F, Tenza-Abril AJ, Baeza FJ, Bañón L. Residual compressive strength of recycled aggregate concretes after high temperature exposure. Materials. 2020;13:1981. doi: 10.3390/MA13081981.
[67] IS 516 (Part 1/Section 1): 2021. Hardened Concrete – Methods of Test. Bureau of Indian Standards, New Delhi, India, 2021. n.d.
[68] IS 516 (Part 5/Section 1): 2018. Hardened Concrete – Methods of Test. Bureau of Indian Standards, New Delhi, India, 2018. n.d.
[69] DIN 1048 (Part-5): 1991. Testing of Hardened Concrete (Specimens Prepared in Mould). Deutsches Institute for Normung: Berlin, Germany, 1991. n.d.
[70] Yuzer N, Akoz F, Ozturk LD. Compressive strength-color change relation in mortars at high temperature. Cem Concr Res. 2004;34:1803–7. doi: 10.1016/j.cemconres.2004.01.015.
[71] Short NR, Purkiss JA, Guise SE. Assessment of fire damaged concrete using colour image analysis. Constr Build Mater. 2001;15:9–15.
[72] He KC, Guo RX, Ma QM, Yan F, Lin ZW, Sun YL. Experimental research on high temperature resistance of modified lightweight concrete after exposure to elevated temperatures. Adv Mater Sci Eng. 2016;2016:1–6. doi: 10.1155/2016/5972570.
[73] Ma Q, Guo R, Sun Y, He K, Du H, Yan F, et al. Behaviour of modified lightweight aggregate concrete after exposure to elevated temperatures. Mag Concr Res. 2018;70:217–30. doi: 10.1680/jmacr.17.00136.
[74] Gong J, Deng G, Shan B. Performance evaluation of RPC exposed to high temperature combining ultrasonic test: A case study. Constr Build Mater. 2017;157:194–202. doi: 10.1016/j.conbuildmat.2017.08.140.
[75] Khoury GA. Compressive strength of concrete at high temperatures: a reassessment. Mag Concr Res. 1992;44:291–309.
[76] Hertz KD. Concrete strength for fire safety design. Mag Concr Res. 2005;57:445–53.
[77] Li M, Qian CX, Sun W. Mechanical properties of high-strength concrete after fire. Cem Concr Res. 2004;34:1001–5. doi: 10.1016/j.cemconres.2003.11.007.
[78] Phan LT, Carino NJ. Effects of test conditions and mixture proportions on behavior of high-strength concrete exposed to high temperatures. ACI Mater J. 2002;99:54–66.
[79] Khaliq W, Taimur. Mechanical and physical response of recycled aggregates high-strength concrete at elevated temperatures. Fire Saf J. 2018;96:203–14. doi: 10.1016/j.firesaf.2018.01.009.
[80] Sachin V, Suresh N. Residual properties of normal-strength concrete subjected to fire and sustained elevated temperatures: A comparative study. J Struct Fire Eng. 2021;12:1–16. doi: 10.1108/JSFE-02-2020-0007.
[81] Hlavička ĚLV. Bond after fire. Constr Build Mater. 2017;132:210–8. doi: 10.1016/j.conbuildmat.2016.11.131.
[82] Aydin S, Yazici H, Baradan B. High temperature resistance of normal strength and autoclaved high strength mortars incorporated polypropylene and steel fibers. Constr Build Mater. 2008;22:504–12. doi: 10.1016/j.conbuildmat.2006.11.003.
[83] Thanaraj DP, Anand N, Prince Arulraj G, Zalok E. Post-fire damage assessment and capacity based modeling of concrete exposed to elevated temperature. Int J Damage Mech. 2020;29:748–79. doi: 10.1177/1056789519881484.
[84] Uysal M, Akyuncu V. Durability performance of concrete incorporating Class F and Class C fly ashes. Constr Build Mater. 2012;34:170–8. doi: 10.1016/j.conbuildmat.2012.02.075.
[85] Singh H, Kumar Tiwary A, Singh S. Experimental investigation on the performance of ground granulated blast furnace slag and nano-silica blended concrete exposed to elevated temperature. Constr Build Mater. 2023;394:132088. doi: 10.1016/j.conbuildmat.2023.132088.
[86] Komonen J, Penttala V. Effects of high temperature on the pore structure and strength of plain and polypropylene fiber reinforced cement pastes. Fire Technol. 2003;39:23–34.
[87] Correia JR, Lima JS, de Brito J. Post-fire mechanical performance of concrete made with selected plastic waste aggregates. Cem Concr Compos. 2014;53:187–99. doi: 10.1016/j.cemconcomp.2014.07.004.
[88] Kore Sudarshan D, Vyas AK. Impact of fire on mechanical properties of concrete containing marble waste. J King Saud Univ - Eng Sci. 2019;31:42–51. doi: 10.1016/j.jksues.2017.03.007.

[89] Bakhtiyari S, Allahverdi A, Rais-Ghasemi M, Zarrabi BA, Parhizkar T. Self-compacting concrete containing different powders at elevated temperatures - Mechanical properties and changes in the phase composition of the paste. Thermochim Acta. 2011;514:74–81. doi: 10.1016/j.tca.2010.12.007.

[90] Ismail M, Elgelany Ismail M, Muhammad B. Influence of elevated temperatures on physical and compressive strength properties of concrete containing palm oil fuel ash. Constr Build Mater. 2011;25:2358–64. doi: 10.1016/j.conbuildmat.2010.11.034.

[91] Ming X, Cao M, Lv X, Yin H, Li L, Liu Z. Effects of high temperature and post-fire-curing on compressive strength and microstructure of calcium carbonate whisker-fly ash-cement system. Constr Build Mater. 2020;244:118333. doi: 10.1016/j.conbuildmat.2020.118333.

[92] Gupta T, Siddique S, Sharma RK, Chaudhary S. Effect of elevated temperature and cooling regimes on mechanical and durability properties of concrete containing waste rubber fiber. Constr Build Mater. 2017;137:35–45. doi: 10.1016/j.conbuildmat.2017.01.065.

[93] Lin Y, Hsiao C, Yang H, Lin YF. The effect of post-fire-curing on strength-velocity relationship for nondestructive assessment of fire-damaged concrete strength. Fire Saf J. 2011;46:178–85. doi: 10.1016/j.firesaf.2011.01.006.

[94] Wróblewski R, Stawiski B. Ultrasonic assessment of the concrete residual strength after a real fire exposure. Buildings. 2020;10:1–13. doi: 10.3390/buildings10090154.

[95] Luo X, Sun W, Yin S, Chan N. Effect of heating and cooling regimes on residual strength and microstructure of normal strength and high-performance concrete. Cem Concr Res. 2000;30:379–83. doi: 10.1016/S0008-8846(99)00264-1.

[96] Nadeem A, Memon SA, Lo TY. The performance of Fly ash and Metakaolin concrete at elevated temperatures. Constr Build Mater. 2014;62:67–76. doi: 10.1016/j.conbuildmat.2014.02.073.